Green Synthesis and Characterization of Zinc Oxide Nanoparticles Using Leaf Extract of *Abies pindrow* Royle and Their Antimicrobial Activity

Shama Parveen¹, Deep Narayana Maurya², Nitin Kumar Agrawal³, Animesh Agarwal³, Manish Saxena³, Shiwali Bisht⁴, Rekha Rikhari¹, Rashmi Yadav⁵, Vikas Gupta¹, Siddhi Jaiswal⁶

¹Department of Chemistry, Faculty of Science, Motherhood University, District- Haridwar, 247661, Uttarakhand, India

²Department of Chemistry, Faculty of Science, DN (P.G.) College, Meerut, 250002, Uttar Pradesh, India

³Department of Applied Sciences and Humanities, Moradabad Instituteof Technology, Moradabad, 244001, Uttar Pradesh, India

⁴Department of Microbiology, Faculty of Science, Motherhood University, District-Haridwar, 247661, Uttarakhand, India

⁵Department of Education, Model Public Education College, Chandausi Sambhal, Moradabad, 244412, Uttar Pradesh, India

⁶Department of Chemistry, Faculty of Science, Shri Venkateshwara University, NH-24, Venkateshwara Nagar, Rajabpur Gajraula, District, Amroha, 244236, Uttar Pradesh, India

Corresponding author- Shamahussainktw@gmail.com

In this study, we describe the environmentally friendly production of zinc oxide nanoparticles (ZnONP) using the coating component *Abies pindrow* Royle Functionalization of ZnONPs from *Abies pindrow* Royle using Scanning Electron Microscopy, X-ray Diffraction, Fourier Transform Infrared Spectroscopy, UV-Vis Absorption and Antibacterial Studies. According to XRD analysis, ZnONPs have an average grain size of 16.47 nm and a wurtzite hexagonal structure. SEM with EDX was used to analyse nanoparticles morphology and content composition. These morphological studies revealed that ZnONPs have a nanorod shape. FT-IR spectroscopy provided further evidence of group activity. The band gap measured in UV-Vis studies is 4.42 eV. The difference in ZnONP size and surface area/volume ratio was found to be the main reason for its importance in antibacterial activity. The antibacterial activity of ZnONPs was evaluated for gram positive (Staphylococcus aureus and bacillus sublitis) and gram negative (Pseudomonas aeruginosa and E. coli) and yeast (candida albicans) using the positive diffusion technique. Antibiotic studies have shown that ZnONPs can inhibit the growth of Gram-positive bacteria, Gram-negative bacteria and yeast. A result shows that the synthesized zinc oxide nanoparticle shows strong activity towards Bacillus sublitis and there is no have potential towards E. coli.

Key words: Green synthesis, zinc oxide nanoparticles, characterization and antibacterial activity.

Introduction

Chemistry, physics, biology, pharmacology and informatics are just a few of the fields where nanotechnology is used (1, 6). Zinc oxide nanoparticles are preferred over other semiconductor materials due to special semiconductor, optical, pyroelectric and piezoelectric properties and biodegradability. ZnONPs is a good n-type semiconductor material with wide band gap (7, 8). The FDA generally classifies zinc oxide as safe (GRAS) due to its low toxicity (9). For this reason, it is used in many disciplines such as beauty products, sensors, food safety, packaging, electronic transistors and catalysis. The widespread industrial use of the antibacterial potential of ZnONP suggests that it may one day effectively and efficiently replace antibiotics (10, 11). Some Physical and chemical methods used to produce ZnONPs of various shapes and sizes include hydrothermal methods, infrared radiation, chemical vapor deposition, spray pyrolysis, and microwave assisted sputtering (12,13). There are many physical and chemical methods available to obtain ZnONPs, most of which are based on nontoxic materials (14, 20). Therefore, to produce metal oxide nanoparticles, a more environmentally friendly, methods should be applied. To date, the most economically, environmentally friendly and efficient application of metal nanoparticles is to use plants or plants products. Green synthesis using plants in nanotechnology have not only been studied. but it has been shown that ZnONPs can be utilized as drugs also (21). Brassica oleracae var, Cymbopogon, Citrus, Viscum album, Pelargonium zonale, Punica granatum, Aegle marmelos, Olea ferruginea and Berberis vulgaris are some examples of plants used to produce leaf extract mediated (22, 29).

Experimental Method

Gathering of plant material

The leaves of *Abies pindrow* Royle were collected from Kotdwar, Uttarakhand, India. Dry leaves were used in the study.

Preparation of Leaf Extract

Abies pindrow Royle were taken out of Kotdwara, where they were living in their natural habitat, then cleansed with ionized water to reduce any dust that remained. The leaves were scrubbed and shorted before being allowed to air dry for three to four days before being milled into a powder. The leaves of this plant were pulverized into a fine powder using a grinding machine, and the powder was stored to be used in the test. To extract the necessary ingredient, 8 grams of *Abies pindrow* Royle powdered leaf were cooked for an hour at 85 to 90° C in a round-bottomed container with a volume of 1000 mL, add 300 mL of water that has been deionized. The brown color of the watery extract solution after an hour is proof that the extract has produced. After remaining at room temperature extract was filtered taking what man No. 1 filter paper into use. Figure 1 depicts a produced leaf extract in a yellow tint.

Chemicals

The solvent and chemical utilized in the investigation, zinc chloride (ZnCl₂) was of purest and most analytical grade and were bought from Sigma Aldrich.

Synthesis of zinc oxide nanoparticles

To produce ZnONPs, a 0.01M aqueous zinc chloride solution was made. After adding 6 ml of *Abies pindrow Royle* leaf extract, stirring was continued for 1 hour and 40 minutes using a magnetic stirrer. The original brown color of the preparation was changed to pale yellow. After the mixture reached room temperature, it was cooled. Centrifuge the solution at 1000 rpm for 15 minutes to form NPs. The product was washed in two cycles of distilled water to remove impurities. ZnONP was saved for later research.

Characterization

Characterization methods assist in understanding the precise characteristics of the nanoparticles to be investigated in an accurate, timely manner that is trustworthy to interpret the calculated values. To better understand their unique properties, the produced ZnONPs were examined by a variety of characterization studies, such as those on their functional groups, size of particles, chemical composition, mechanical, electronic, structural, morphological, and atomic composition. These analyses could be made precisely using advanced techniques like UV-VIS spectroscopy. (Jasco V650), zeta potential, Zeta sizer (Malvern make), and XRD (Bruker D8 Advanced equipped with Cu, K-alpha radiation source), FT-IR (Shimadzu, IR affinity 1A) and SEM (JEOL JEM 2100, Japan) instruments. EDX (AMETEK team V.4.3 EDS detector). These techniques enabled us to verify that our technique is correctly optimized and matches the requirements specified.

Antimicrobial Activity

To explore potential therapeutic uses of ZnONPs for antibiotic use, we investigated the antimicrobial properties of ZnONPs for antibiotic use; we investigated the antibacterial properties of ZnONPs. Bacterial resistance was measured using positive agar smears as reported elsewhere. For the antibiotic test, Staphylococcus aureus, Bacillus subtilis, Pseudomonas aeruginosa, Escherichia coli and Candida albicans were used.

Well Diffusion Method

A bacterial strain was grown in Muller-Hinson medium for an entire night at 37°C. The inoculum was calibrated using a sterile saline and the CLSI (clinical and laboratory standard institute) guidelines to get the desired density of 0.5 McFarland standard (1.5 x 108 CFU/mL). To achieve complete absorption, microbial inoculum was evenly distributed across the tops of plates containing growth environment and kept at room temperature for 15 minutes. Using a sterile cork barer, 7 mm-diameter holes have been aseptically punched onto inoculation plates, and 50 ul of a nanoparticles solution has been added to each well. After that, bacteria-filled agar plates were incubated at 37°C for 24 hours in accordance with the diameter (mm) of the inhibitory zones that develop as a result of the diffusion of Schiff bases in the medium and the

inhibition zones of microbial progress, the antimicrobial activity of produced nanoparticles were assessed.

UV. Visible Spectrum

UV-Vis spectroscopy is often used to characterize the optical properties of Visible ZnONPs. Figure 2. UV-Vis absorption spectra of the synthesized nanoparticles were observed. It is clearly seen that the band gap absorption of ZnONPs caused by electron transfer between conduction and valence bands has an absorption peak at 280 nm. These studies provide further evidence that zinc ZnONP is produced from *Abies pindrow* Royle leaf extracts. ZnONPs were found to have band gap energy of 4.42 eV. Internal defects such as oxygen vacancies and zinc interstitials that generate local electrons at different energies are thought to be responsible forthe reduced band gap values.

FT-IR

To investigate the reduction potential, FT-IR spectroscopy measurements of changes in functional group binding due to ZnONPs and *Abies pindrow* Royle extracts were performed asshown in Figure 3. The absorption peaks at 3672 cm⁻¹ and 3057 cm⁻¹ are related to stretching vibrations of hydroxyl (OH) groups. The other peaks in the FTIR spectrum are at 2094 cm⁻¹, 1680 cm⁻¹, 852 cm⁻¹ and 744 cm⁻¹, which correspond to stretching of the C=C bonds of the alkynes and amide carbonyl functional groups C=O contract.

Peaks below 771 cm⁻¹ represent Zn-O bonds. The above studies show that ZnO interacts positively with secondary metabolites in plants. These data suggest that biochemical such as phenolic compounds and flavonoids may contribute to reduction and stabilization during ZnONP synthesis.

XRD

The ZnONPs pattern from XRD is shown in Figure 4. The XRD peaks clearly expand, which suggests that the substance produced comprises nanoscale-sized particles. We analyzed the XRD patterns and calculated the maximum intensity, location, and width using full-width at half-maximum data. Lattice constants a = b = 0.324 nm and the diffraction maxima are at 31.23 and 34.03 and c = 0.521 nm has been specifically identified as the hexagonal wurtzite phase of ZnONPs (JPCDS card number: 36-1451). The Debye-Scherrer formula was used to calculate the diameter of the synthesized ZnONPs. The full width at half-maximum of the diffraction peak related to the plane at 100,002, 102, 200, and 112. Analysis showed that the sample's average size was 16.47 nm (30).

Morphology of ZnONPs

SEM images are used to make predictions regarding the morphology of ZnONPs figure 5 shows nanorod shaped SEM images of ZnONPs with various magnifications. Synthesized zinc oxide is nanorod in shape (31). According to the examination utilizing EDX analysis, ZnONPs are metallic and have a crystalline structure. EDAX was used to calculate the weight percentages of zinc (51.28%), oxide (39.41%), and other elements (9.31%).

..

Results and Discussion

UV. Visible Spectrum

UV-Vis spectroscopy is often used to characterize the optical properties of Visible ZnONPs. Figure 2. UV-Vis absorption spectra of the synthesized nanoparticles were observed. It is clearly seen that the band gap absorption of ZnONPs caused by electron transfer between conduction and valence bands has an absorption peak at 280 nm. These studies provide further evidence that zinc ZnONP is produced from *Abies pindrow* Royle leaf extracts. ZnONPs were found to have band gap energy of 4.42 eV. Internal defects such as oxygen vacancies and zinc interstitials that generate local electrons at different energies are thought to be responsible forthe reduced band gap values.

FT-IR

To investigate the reduction potential, FT-IR spectroscopy measurements of changes in functional group binding due to ZnONPs and *Abies pindrow* Royle extracts were performed asshown in Figure 3. The absorption peaks at 3672 cm⁻¹ and 3057 cm⁻¹ are related to stretching vibrations of hydroxyl (OH) groups. The other peaks in the FTIR spectrum are at 2094 cm⁻¹, 1680 cm⁻¹, 852 cm⁻¹ and 744 cm⁻¹, which correspond to stretching of the C=C bonds of the alkynes and amide carbonyl functional groups C=O contract.

Peaks below 771 cm⁻¹ represent Zn-O bonds. The above studies show that ZnO interacts positively with secondary metabolites in plants. These data suggest that biochemical such as phenolic compounds and flavonoids may contribute to reduction and stabilization during ZnONP synthesis.

XRD

The ZnONPs pattern from XRD is shown in Figure 4. The XRD peaks clearly expand, which suggests that the substance produced comprises nano scale-sized particles. We analyzed the XRD patterns and calculated the maximum intensity, location, and width using full-width at half-maximum data. Lattice constants a = b = 0.324 nm and the diffraction maxima are at 31.23, 34.03 and c = 0.521 nm has been specifically identified as the hexagonal wurtzite phase of ZnONPs (JPCDS card number: 36-1451). The Debye-Scherrer formula was used to calculate the diameter of the synthesized ZnONPs. The full width at half-maximum of the diffraction peak related to the plane at 100,002, 102, 200, and 112. Analysis showed that the sample's average size was 16.47 nm (30).

Morphology of ZnONPs

SEM images are used to make predictions regarding the morphology of ZnONPs figure 5 shows nanorod shaped SEM images of ZnONPs with various magnifications. Synthesized zinc oxide is nanorod in shape (31). According to the examination utilizing EDX analysis, ZnONPs are metallic and have a crystalline structure. EDAX was used to calculate the weight percentages of zinc (51.28%), oxide (39.41%), and other elements (9.31%).

..

Zeta potential Analysis zinc oxide nanoparticles (ZnONPs)

The charge stability of ZnONPs produced from *Abies pindrow Royle* leaf extract can be analyzed using the Zeta potential. The zeta capability denotes the charge on the surface. Figure 6. Demonstrate the zeta potentials of ZnONPs dispersed in water were decided to be -17.71mV. Zeta potential at its maximum clearly shows good stability.

Antimicrobial Activity

Table 1. Shows the inhibition zones for nanoparticles of zinc oxide produced using the Agar well diffusion method

1	Concentration of ZnONPs	Staphylococcus aureus Inhibition zone (mm)	Bacillus subtilis Inhibition zone (mm)	Escherichia coli. Inhibition zone (mm)	Pseudomonas aeruginosa inhibition zone (mm)	Candida albicans Inhibition zone (mm)
		13	19	NI	11	12

NI = No inhibition zone

It was noted that the values of the inhibitory zones for Gram-positive (staphylococcus aureus and Bacillus subtilis), Gram-negative bacteria (E. coli and Pseudomonas aeruginosa) and yeast (candida albicans). Bacteria were recorded for ZnONPs that were created from the leaf extract of Abies pindrow Royle which is shown in table 1. As demonstrated in Figure 4. ZnONPs significantly reduced yeast and bacterial development. The 19 mm showed a maximum zone of inhibition for Bacillus subtilis. However, the results of our study on antimicrobial activity showed that antimicrobial activity increased with increasing ZnONPs concentration, and revealed the species specificity affected the zone of inhibition and ZnONPs size had a significant impact on antimicrobial activity because of its high surface-to-volume ratio. Additionally, the ribosomal subunit, intercellular, and bacterial cell wall structure are all connected to antibiotic action. By electrostatic interaction, ZnO nanoparticles that are positively charged and negatively charged bacteria can bind. As a result, cell wall bound ZnONPs induce the microbial cell wall to develop pith and lose the integrity of the cell membrane (Umavathi et al., 2020; Kim et al., 2020; Viswanathan et al., 2020). The main causes of microbial cell death are out-of-balance metabolic processes and biological electrolyte leaking (32). Studied show that the synthesized zinc oxide nanoparticles have no potential to inhibit the growth of E. coli bacterial on the other hand ZnONPs show strong activity towards Bacillus sublitis (figure 7).

Conclusion

The green synthesis of ZnONPs is widely acknowledged to be substantially safer and more environmentally friendly than chemical production. *Abies pinrow royle* was used as the capping agent in the current experiment, and we have detailed the green synthesis of ZnONPs. *Nanotechnology Perceptions* **20 No. 6** (2024)

••

The synthesis of ZnONPs utilizing the leaf extract of *Abies pinrow royle* is confirmed by the XRD patterns. The hexagonal wurtzite structure of ZnONPs and the diffraction peaks are nicely matched. ZnONPs were found to have an average particle size of 16.47 nm. FT-IR spectroscopy was used to analyse the stretching and interactions. The sample displays a distinct and highly detected absorption edge at 280 nm, which is in agreement with the UV-Vis absorption research and points to a red shift in the UV region. 4.42 eV was discovered to be the bandgap value. On the ZnONPs treated plate, antibacterial activity was seen. Staphylococcus aureus and Bacillus Subtilis, E. coli, Pseudomonas aeruginosa and candida albicans plates showed a distinct zone of inhibition at 50µl. In contrast to all bacteria P. aeruginosa and E. coli, significantly more responsive towards ZnONPs. According to the results, ZnONPs can be utilized to coat surgical instruments for aseptic procedures in the medical industry since they prevent the growth of both pathogenic and normal bacteria.

References

- 1. A. L. Porter, J. Youtie, J. Nanopart. Res., 11, 1023–1041 (2009).
- 2. M. Govindarajan, G. Benelli, Ecotoxicol. Environ. Saf., 133, 395–402 (2016).
- 3. M. Govindarajan, G. Benelli, J. Clust. Sci., 28, 15–36 (2017).
- 4. C. Balalakshmi, K. Gopinath, M. Govindarajan, R. Lokesh, A. Arumugam, N. S. Alharbi, S. Kadaikunnan, J. M. Khaled, G. Benelli, J. Photochem. Photobiol B, 173, 598–605 (2017).
- 5. M. Divya, B. Vaseeharan, M. Abinaya, S. Vijayakumar, M. Govindarajan, N. S. Alharbi, S. Kadaikunnan, J. M. Khaled, G. Benelli, J. Photochem, Photobiol B **178**, 211–218 (2018).
- 6. B. A. Fahimmunisha, R. Ishwarya, M. S. AlSalhi, S. Devanesan, M. Govindarajan, B. Vaseeharan, J. Drug Deliv. Sci. Technol., 55. (2020)
- 7. D. Suresh, R.M. Shobharani, P.C. Nethravathi, M.A.P. Kumar, H. Nagabhushana,141, 128–134 (2015).
- 8. R. Gill, S. Ghosh, A. Sharma, D. Kumar, V.H. Nguyen, D.V.N. Vo, T.D. Pham, P. Kumar, Mater. Lett., 277, 128295 (2020).
- 9. M. Chennimalai, V. Vijayalakshmi, T.S. Senthil, N. Sivakumar, Mater. Today., 47, 1842–1846 (2021).
- 10. A. Krol, V. Railean-Plugaru, P. Pomastowski, B. Buszewski, Phytochem. Lett., 31, 170–180 (2019).
- 11. H. Singh, A. Kumar, A. Thakur, P. Kumar, V.H. Nguyen, D.V.N. Vo, A. Sharma, D. Kumar, Top. Catal., 63, 1097–1108 (2020).
- 12. D. Skoda, P. Urbanek, J. Sevcik, L. Munster, J. Antos, I. Kuritka, Mater. Sci. Eng. B., 232–235, 22–32 (2018).
- 13. S. Bhat, S.V. Shrisha, K.G. Naik, Arch. Phy. Res., 4, 61–66 (2013).
- 14. S. S. Kumar, P. Venkateswarlu, V. R. Rao, G. N. Rao, G.N, Int. Nano Lett., 3, 30 (2013).
- 15. P. Suganya, B. Vaseeharan, S. Vijayakumar, B. Balan, M. Govindarajan, N. S. Alharbi, S. Kadaikunnan, J. M. Khaled, G. Benelli, J. Photochem. Photobiol B., **173**, 404–411 (2017).
- 16. R. Ishwarya,B. Vaseeharan, R. Anuradha, R. Rekha, M. Govindarajan, N. S,Alharbi, S. Kadaikunnan, J. M. Khaled, G. Benelli,J. Photochem. Photobiol B., 174, 133–143 (2017a).
- 17. R. Thaya, B. Vaseeharan, J. Sivakamavalli, A. Iswarya, M. Govindarajan, N. S. Alharbi, S. Kadaikunnan, M. N. Al-anbr, J. M. Khaled, G. Benelli, Microb. Pathoge., 114, 17–24 (2018).
- 18. V. Karthika, M.S. AlSalhi, S. Devanesan, K. Gopinath, A. Arumugam, M. Govindarajan, Sci. Rep., 10, 1 (2020). G. Kasi, J. Seo, Influence of Mg doping on the structural, 2019

- 19. R. M. Kiriyanthan, S. A. Sharmili, R. Balaji, S. Jayashree, S.Mahboob, K. A. Al-Ghanim, F. Al-Misned, Z. Ahmed, M. Govindarajan, B. Vaseeharan, Photodiagn. Photodyn. Thar.,32
- 20. M. MuthuKathija, M. S. M. Badhusha, & V. Rama, V., Applied Surface Science Advances., 15, 100400 (2023).
- 21. H. S. Elshafie, A. Osman, M. M. El-Saber, J. Camele, I., & E. Abbas, The Plant Pathology Journal., 39(3), 265 (2023).
- 22. U. Manojkumar, D. Kaliannan, V. Srinivasan, B. Balasubramanian, H. Kamyab, Z. H. Mussa, & S. Palaninaicker, S, Chemosphere., 323, 138263, (2023).
- 23. Y. H. I.Mohammed, S. Alghamdi, H. A. Alzahrani, B. Jabbar, D. Marghani, S. Beigh & W. N. Hozzein, ACS Omega., (2023).
- 24. W. Mushtaq, M. Ishtiaq, M. Maqbool, M. W. Mazhar, R. Casini, A. M. Abd-ElGawad, & H. O. Elansary, Plants., 12(11), 2130 (2023).
- 25. A. Vahidi, H. Vaghari, Y. Najian, M. Najian, H. Jafarizadeh-Malmiri, H, Green Process. Synth., 8, 302–308 (2019).
- 26. E. Karaköse, H. Çolak, F. Duman, F, Green Process. Synth., 6, 317–323 (2017).
- 27. J. Fowsiya, I. V. Asharani, S. Mohapatra, A. Eshapula, P. Mohi, N. Thakar, S. Monad, G. Madhumitha, Green Process Synth., **8**, 488–495 (2019).
- 28. A. Hussain, A. Mehmood, G. Murtaza, K. Ahmad, A., Ulfat, M. Khan, T. Ullah, T, Green Process. Synth., 9, 451–461 (2020).
- 29. Y. Anzabi, Green Process. Synth., 7, 114–121 (2018).
- 30. I. Kim, K. Viswanathan, G. Kasi, K. Sadeghi, S. Thanakkasaranee, J. & Seo, Polymers,, 11(9), 1427 (2019).
- 31. Y., L., A. Uddin, H. Wang. Nanomaterials and Nanotechnology 5 (2015): 19.
- 32. K., I., K. Viswanathan, G. Kasi, K. Sadeghi, S. Thanakkasaranee, J. Seo. Polymers 11, no. 9 (2019): 1427.

Figures



Figure 1: Synthesized leaf extract of *Abies pindrow* Royle



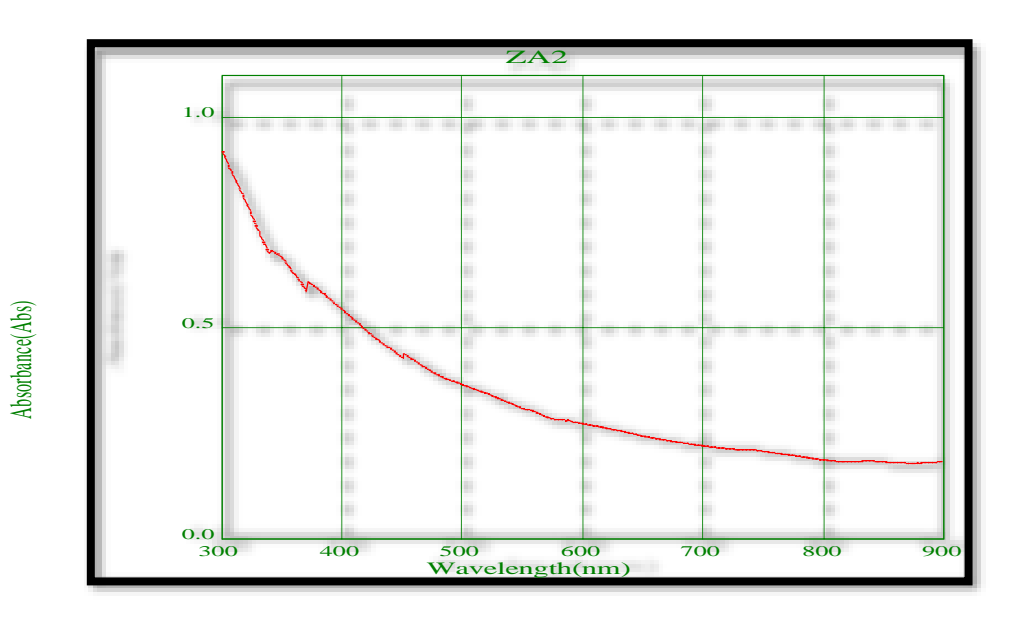


Figure 2: UV. Visible spectra of synthesized zinc oxide nanoparticles

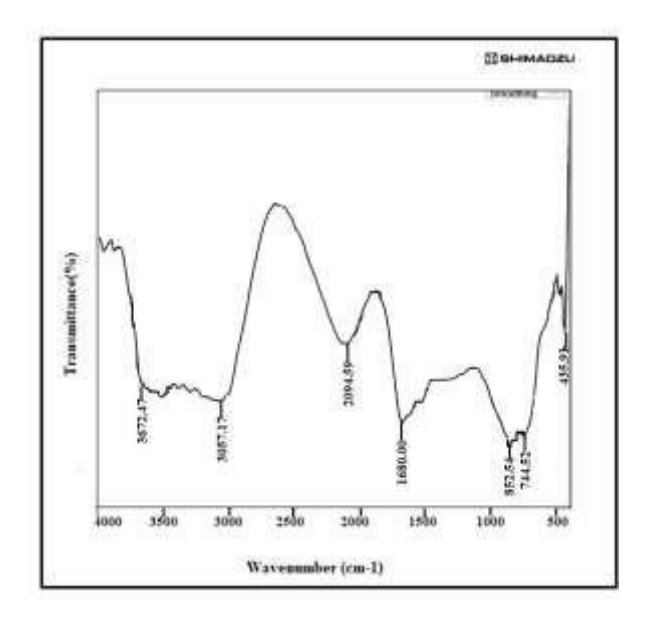


Figure 3: FTIR spectra of synthesized Zinc oxide nanoparticles

••

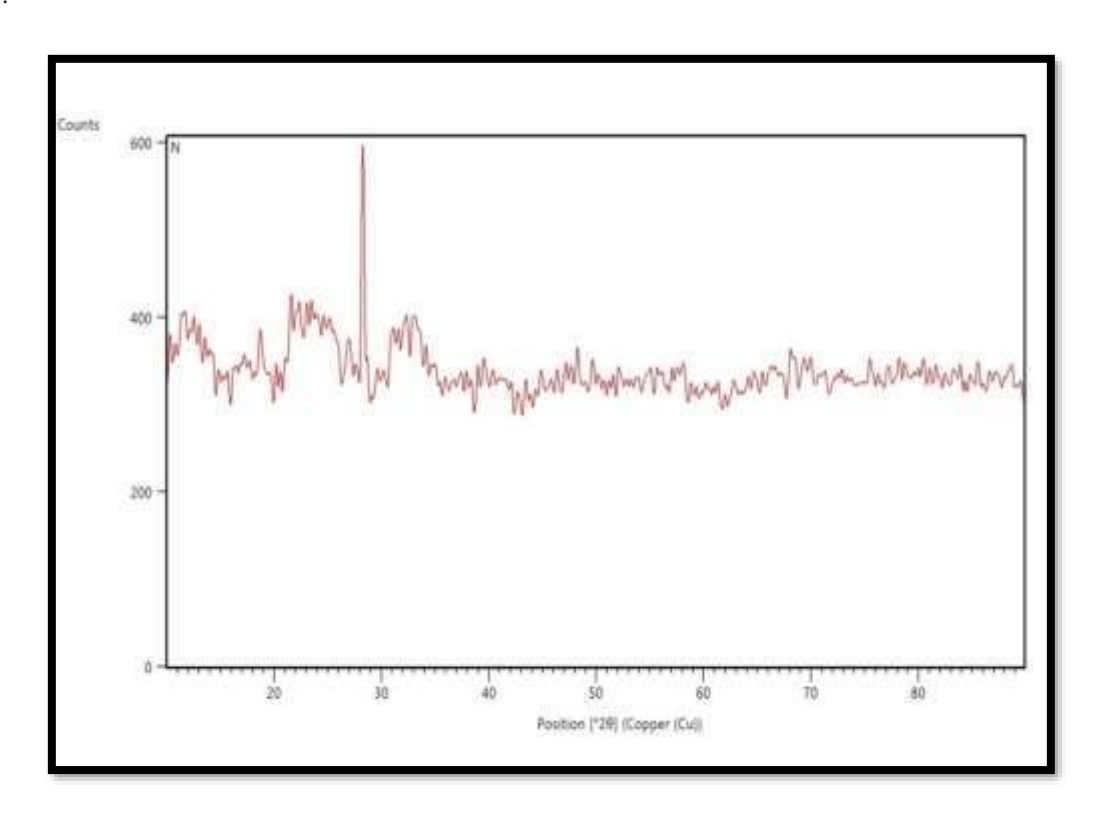


Figure 4: XRD spectra of synthesized Zinc oxide nanoparticles

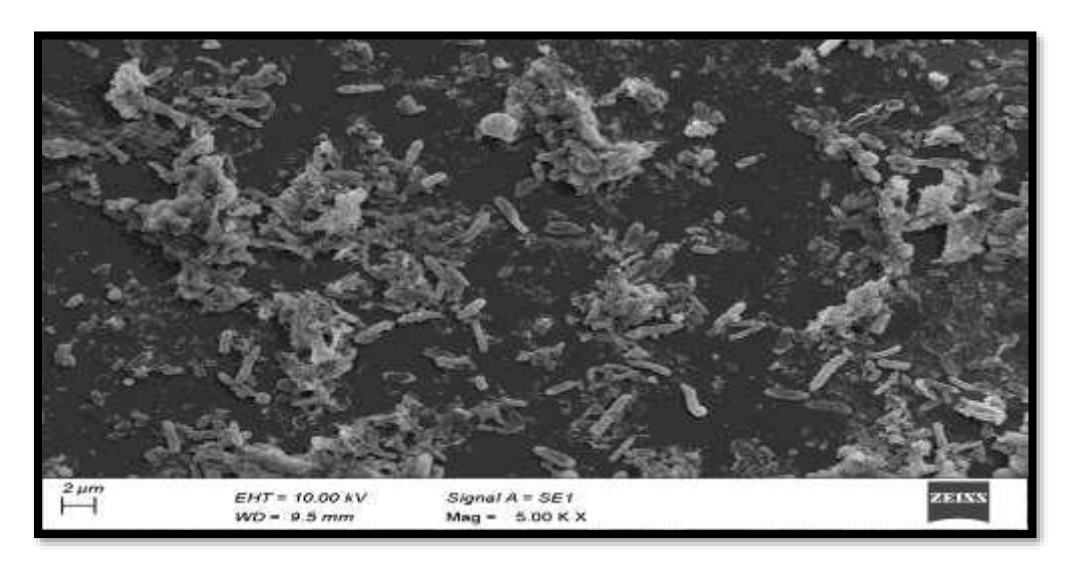


Figure 5: Depicts the SEM image of Zinc oxide nanoparticles made from $Abies\ pindrow\ Royle$ leaf extract using 5.00 KX

Nanotechnology Perceptions 20 No. 6 (2024)



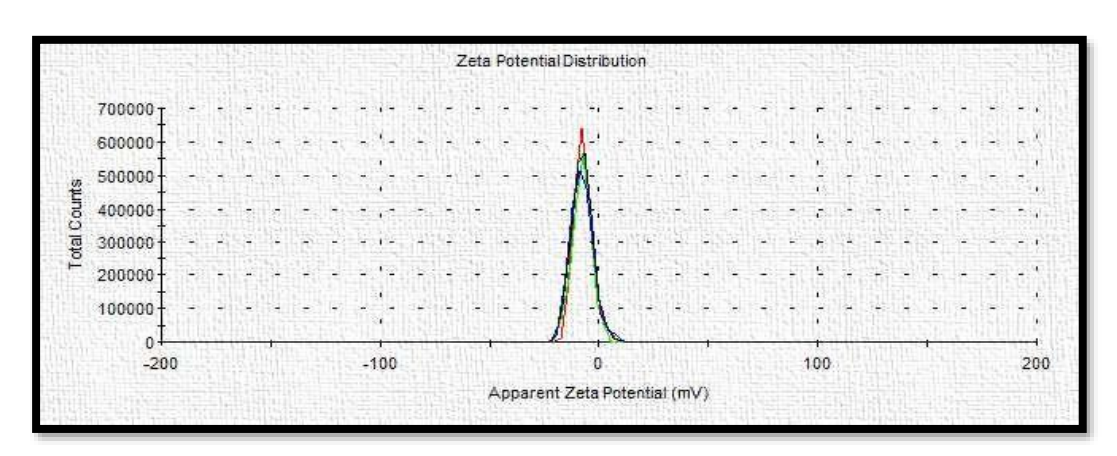


Figure 6: Zeta potential of ZnONPs

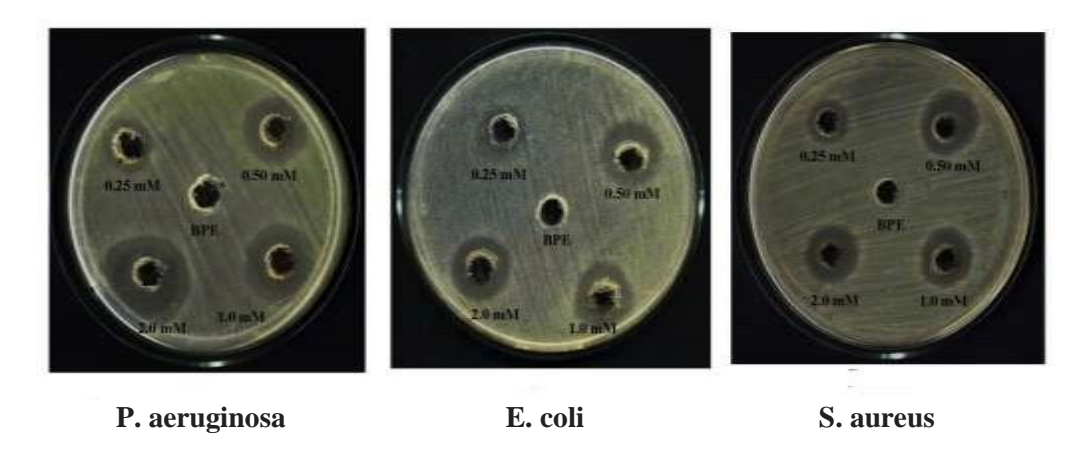


Figure 7: Zone of inhibition of ZnONPs against (a) Pseudomonas aeruginosa (b) Escherichia coli. (c) Staphylococcus aureus